



Deposited via The University of Sheffield.

White Rose Research Online URL for this paper:

<https://eprints.whiterose.ac.uk/id/eprint/94579/>

Version: Accepted Version

Article:

Tronci, G. and Marshall, M.B. (2016) Understanding the Behaviour of Silver as a Low Friction Coating in Aerospace Fasteners. *Tribology International*, 100. pp. 162-170. ISSN: 1879-2464

<https://doi.org/10.1016/j.triboint.2015.12.050>

Article available under the terms of the CC-BY-NC-ND licence
(<https://creativecommons.org/licenses/by-nc-nd/4.0/>)

Reuse

This article is distributed under the terms of the Creative Commons Attribution-NonCommercial-NoDerivs (CC BY-NC-ND) licence. This licence only allows you to download this work and share it with others as long as you credit the authors, but you can't change the article in any way or use it commercially. More information and the full terms of the licence here: <https://creativecommons.org/licenses/>

Takedown

If you consider content in White Rose Research Online to be in breach of UK law, please notify us by emailing eprints@whiterose.ac.uk including the URL of the record and the reason for the withdrawal request.

UNDERSTANDING THE BEHAVIOUR OF SILVER AS A LOW FRICTION COATING IN AEROSPACE FASTENERS

Authors:

Giuseppe Tronci, University of Sheffield, UK – gtronci1@sheffield.ac.uk

Dr Matthew B. Marshall, University of Sheffield, UK – m.b.marshall@sheffield.ac.uk

Abstract

Nuts and bolts used in aero-engines are manufactured from heat-resistant super-alloys. When used in a like on like couple, these materials have a high coefficient of friction, and frequently seizure occurs. In order to prevent this, a silver coating is applied to the nut threads, providing a low friction boundary at the interface. Additionally, a radial crimp is applied to the nut, in order to provide a self-locking feature preventing vibration self-loosening.

In this study, the coefficient of friction of the thread contact will be investigated both during initial joint assembly, and after thermal ageing. Additionally, a finite element model will be employed to investigate the contact mechanics as a consequence of the crimp.

The low coefficient of friction observed during initial assembly was found to be a consequence of shear flow of the silver coating, with an approximate doubling of this value once the coating aged. Areas of silver removal were found to be coincident with areas of high contact pressure in the joint, attributable to the crimp feature.

Keywords

Friction, Self-lubricating, Coating.

1 Introduction

Mechanical components in aero-engines operate over a temperature range from -50 to 760°C . As a consequence the fasteners used to join components together are manufactured from heat resistant super-alloys. When used in a like couple super-alloys have high coefficients of friction, and seizure frequently occurs. To prevent this, a silver coating is normally placed on the nut threads. Additionally, in order to avoid vibration loosening, a radial crimp is added to the end of the nut providing a self-locking feature. Unfortunately, this also has the effect of localizing the contact stresses in two small areas, increasing the risk of removing the silver coating from the nut threads and triggering seizure. Whilst seizure of the joints is undesirable, transfer of removed silver from the nuts to other parts of the engine is a significant issue. In particular, silver can combine with corrosive species in the presence of moisture and attack Ni and Ti alloys leading to an increased inspection requirement.

When a bolted joint is assembled and a load supported, the bolt is elongated. Additionally, due to the helical nature of the thread contact, a moment exists which seeks to unscrew the bolt, and is resisted by thread friction [1]. The problem of self-loosening due to vibration was first identified by Junker [2], where it was highlighted that when a shear load was applied to the joint in a given direction exceeding the friction force, the joint would now be free of friction in all directions. This topic area has subsequently been investigated in multiple studies, with Pai & Hess [3] notably identifying that vibration loosening occurs as a

consequence of localised slip at the thread face. In order to counteract this phenomenon, a variety of self-locking devices have been developed and investigated. These have included, spring washers, double nuts, adhesives and thread inserts, all having varying strengths and weaknesses. As highlighted by Martinez et al. [4] and Petrova et al [5], adhesives are very sensitive to temperature changes and are not reliable if subjected to multiple assemblies. Similarly, Kumar [6], investigated Nylock nuts, which use a nylon collar to increase the coefficient of friction. However, this type of locking feature is only applicable to applications with an operating temperature lower than the melting point of nylon (150°C)[7]. Furthermore, jam nuts and double nuts increase the joint weight, being problematic when large volumes of bolts are utilised [1]. As a consequence, in applications with harsh environments, such as those found in the aerospace industry, fasteners with a mechanical locking feature are frequently used, where the nut is physically deformed providing a clamping effect when the bolt is tightened.

As highlighted, when joints are used in harsh environments, both the nut and bolt are manufactured from Nickel based super-alloys such as Inconel and Waspaloy. These materials have high resistance to creep, high yield stresses and a tensile strength above 1000MPa, and are capable of sustaining high loads at elevated temperatures. Furthermore, they are corrosion and oxidation resistant, with the potential to further improve their properties through different heat treatments [8]. On the other hand, they have high coefficients of friction when used in a like on like couple, as high as 0.6-0.8 if unlubricated, leading to seizure at high contact pressures [8].

In order to prevent seizure when using these materials in like on like couples, lubricants and thin coatings are applied. For example, Houghton et al. [9] investigated the use of DLC coatings in a sliding wear test, and demonstrated a significant reduction in seizure, although this improvement was found to be sensitive to the alloy composition of the substrate used. In this application, as in many bolted joint applications, silver coatings have been used as both a corrosion inhibitor and a dry lubricant [10]. Silver belongs to a family of soft coatings, and can easily shear to reduce friction to as little as 0.1-0.15. Yang et al [11], further investigated three wear regimes: mild, moderate and severe wear, where the coefficient of friction was found to gradually increase for the coating as it sustained increased levels of damage. Furthermore, El Sherbini et al [12] analysed different coating methods, and found ion-plating to be the most satisfactory for Tribology applications. However, electroplating is preferred in various applications due to its cost effectiveness [13]. At present these studies have not investigated the behaviour of silver coatings in bolted joints, despite this type of coating being widely used in the aerospace industry, and also frequently in conjunction with a crimp feature.

In this study the mechanical behaviour of the silver coating has been investigated both experimentally and through Finite Element Modelling. An experimental test platform is developed to investigate the coefficient of friction of crimped fasteners during tightening to an end load of 11.6 kN. The performance of the silver coating is investigated over a period of 6 re-uses, and its durability assessed. Removal of silver in the joint, and the associated contact pressures required for this to occur, are then further analysed through a Finite Element Modelling approach. Following on from this, samples were aged at 760°C for 50 hours, and the coefficient of friction post-test analysed.

2 Methodology

2.1 Test Specimens

Fasteners used in the aerospace industry manufactured from heat resistant super alloys were investigated in this study. As shown in Figure 1, the joint comprised of a simple nut and bolt, with a radially crimped locking feature applied to the chimney of the nut through a clamping vice. The nut, currently in use in engine applications, was 6.35 mm in diameter (1/4") and manufactured from Inconel 718. Additionally, it had a UNF 28 TPI thread form, which had been electroplated with a silver coating to a nominal 5-10 microns thickness. The crimp on the chimney section was also measured and found to reduce the diameter of this section by 0.35mm. The bolt used to assemble the joint had a matching diameter and thread form, and was manufactured from Waspaloy.



Figure 1: Specimens

2.2 Test platform

Figure 2 shows the test platform used to test the silver coated joints. A motor, fixed on the table, turns the nut onto the bolt, compressing the load cell which measures the clamp force. The bolt is situated in a torque sensor, which in turn measures the reaction torque. The load cell is donut shaped, and has the form of a thick washer with a 1/4" diameter hole in the middle, a maximum capacity of 22kN and an accuracy of 0.15kN. The torque sensor is a reaction sensor, with a maximum capacity of 100Nm and an accuracy of 0.2Nm, which is free to move in all directions as it is mounted on a frictionless aluminium guide, to prevent undesired misalignment. The load cell, torque sensor and motor are connected to a computer station, so that load, torque and position are continuously recorded in a text file at a sampling rate of 1000Hz and analysed during postprocessing. A steel washer is also included in the set-up, ensuring that the load is applied on the correct face of the load cell. Finally, a thrust needle bearing is placed under the bolt head, to minimise under head friction during the test, with the frictional resistance of the bearing also previously characterised.

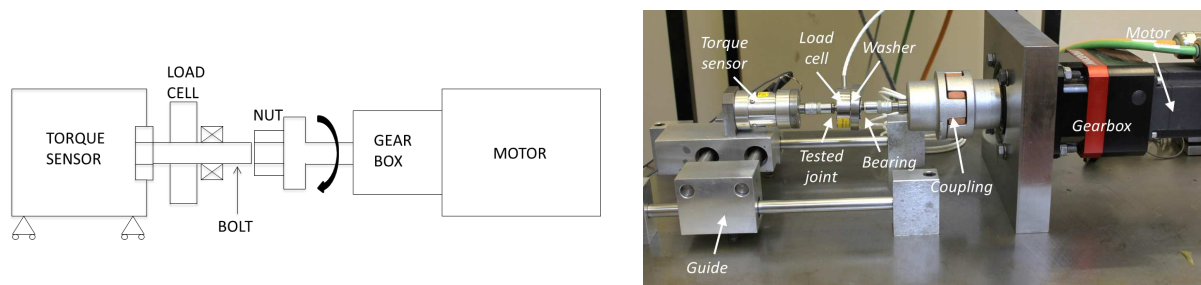


Figure 2: Test Rig

The under head friction torque is one of the four values responsible for the total torque. As shown in Equation 1, the torque required to tighten a joint can be broken down, and is the sum of the clamp or pitch torque, the thread friction torque, the under head friction torque,

and the self-locking torque, also known as break-away torque, defined as the torque necessary to screw a locking device [14].

$$T_{tot} = T_{pitch} + T_{threads} + T_{under\ head} + T_{self\ lock} \quad (1)$$

Assuming that the thread pitch and other geometrical parameters are known, along with the coefficients of friction both on the threads (μ_1) and under the head (μ_2), the total torque required to tighten a joint becomes:

$$T_{tot} = F \left(\frac{P}{2\pi} + \frac{r_1\mu_1}{\cos\beta} + r_2\mu_2 \right) + T_{self-lock} \quad (2)$$

where F is the clamp load, P is the thread pitch and r_1 , r_2 and β are geometrical factors [14]. In this study, the under-head friction is zero through subtraction of the bearing torque, and the locking torque is similarly known, as it is the resisting torque during the screwing on process before the clamping load is applied. Equation 2 can then be simplified to give a relationship between thread friction, thread torque, load, and geometry, and becomes:

$$\mu = \frac{\cos\beta}{r_1} \frac{T_{thread}}{Load} \quad (3)$$

2.3 Test Procedure

2.3.1 Cold Use

As highlighted, during engine assembly joints are typically assembled and reassembled multiple times, with 6 re-uses being a common target. Thus, 6 re-uses have been performed on an as new joint, with an end load of 11.6kN targeted. This end load was selected as it reflects a common design standard for joints of this size in the aerospace industry. Mobil Jet Oil II was applied to the bolt prior to assembling the joint, and a thrust bearing used to isolate the thread torque as previously described. The joints were assembled at rotational speeds of 3rpm during screwing on and off and 0.5rpm during final tightening, in order to achieve a satisfactory accuracy with respect to the targeted clamping load. Torque along with end load was recorded enabling the coefficient of friction to be calculated for each re-use. The test procedure is summarised in Figure 3.

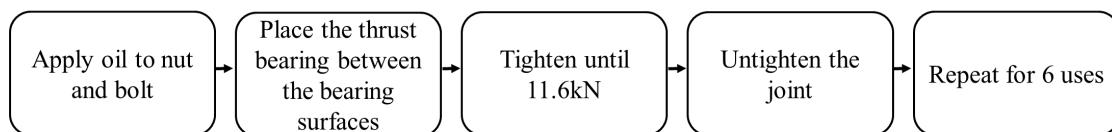


Figure 3: Flowchart of the Cold Test Procedure

2.3.2 Thermal Ageing

During engine operation, the joints must operate at high temperatures, up to 760°C, which can cause the coating to deteriorate and the joint to seize. Thus, assembled joints have been thermally aged at 760°C for 50 hours, and their ability to prevent seizure investigated at room temperature post-cooling. Whilst in the practical application, a significant level of vibration accompanies engine operation, this has not been considered in this case. The aim of this study is to consider a worst case seizure event, and in the case of vibrations these are likely to reduce the level of seizure experienced, and have thus not been included here. In order to

prepare these samples for ageing, the torque required to reach the end load of 11.6kN was first evaluated using the load cell, and the joint then re-assembled with a Waspaloy spacer replacing the load cell (Figure 4 **Error! Reference source not found.**). Re-assembling the joint, the same torque was used, as the room temperature test highlighted no significant difference between the first and the second tightening curve. The Waspaloy spacer had similar dimensions to the load cell, and was used as the load cell could not withstand the ageing process. Mobil Jet Oil II was once again used as a lubricant. The joints were then thermally cycled, and after cooling down to room temperature, unscrewed on the test rig. The torque profile was once again measured. As the load cell was not in place, the coefficient of thread friction was calculated using the torque as the joint began to unscrew, i.e. where the joint load was known. It should also be noted, that the spacer plate was also rotated with the joint inserted in the torque sensor, so the surface torque could be estimated and subtracted. Once disassembled, the joints were re-tested using the load cell, as described previously, in order to fully characterise the coefficient of thread friction using Equation 3, with the overall test procedure summarised in Figure 5.

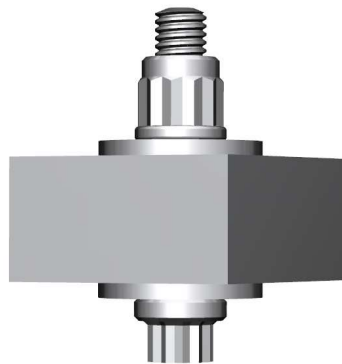


Figure 4: Thermal Ageing Test Spacer

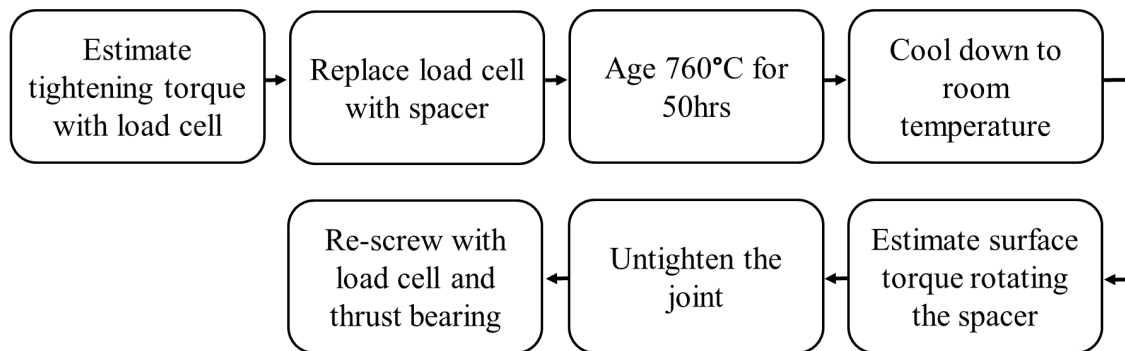


Figure 5: Flowchart of the Thermal Test Procedure

3 Results

During the cold test the torque and the load were acquired continuously during the tightening and un-tightening cycles. Upon post-processing, using the equations previously described, the coefficient of thread friction was isolated and plotted for all 6 re-uses, along with the clamping load (Figure 6).

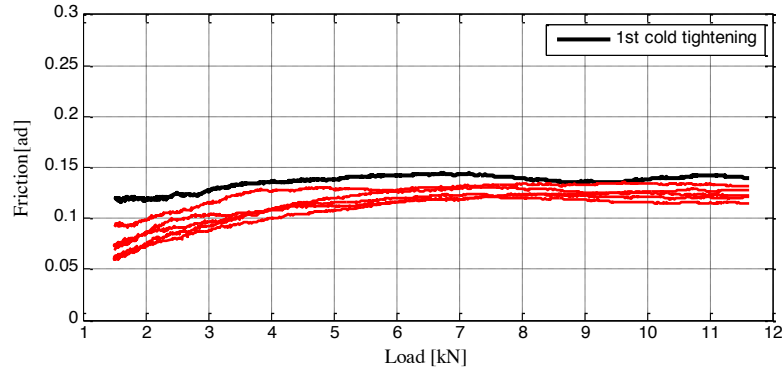


Figure 6: Coefficient of Friction for Cold Re-Uses

As shown in Figure 6, the thread friction over the cycle was found to be between 0.1-0.14, and show a gradual increase with clamping load. Furthermore, the friction during the first tightening was found to be slightly higher with respect to the following re-uses.

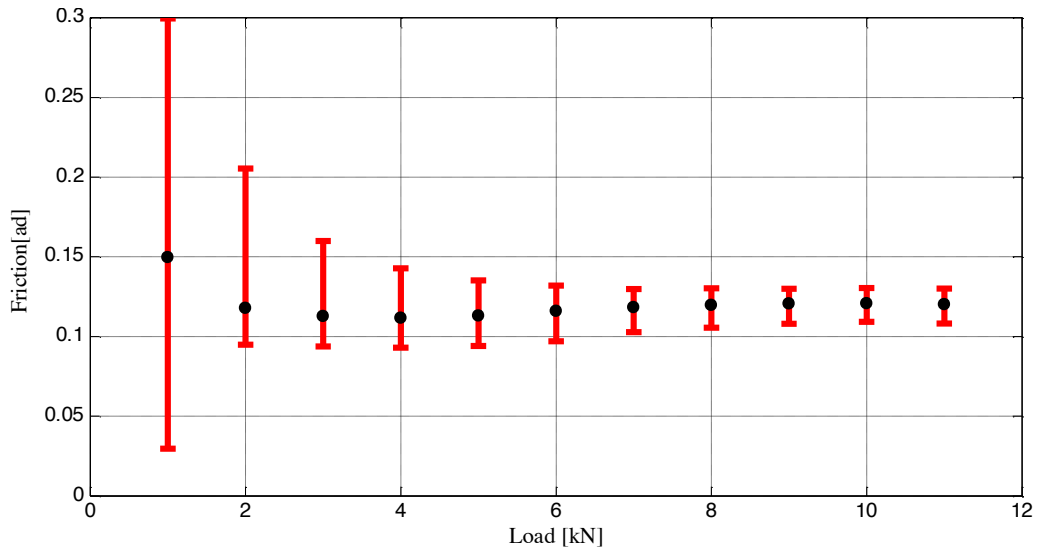


Figure 7: Coefficient of friction for Cold Re-Uses, 5 Tests

Figure 7 shows the average coefficient of thread friction for 5 joints, taking account of the minimum and the maximum value for every 1kN of clamping load. As shown in the figure, the coefficient of friction results show some scatter at low load, with this attributable to the accuracy of the sensors at low values. Also, the self-locking torque was estimated as previously described, and at a low clamping load was a significant part of the total torque (Equation 1). As highlighted in Figure 7, the scatter decreased along with the clamping load, with a value of 0.11-0.13 at end load.

| Before Thermal Ageing | | | After Thermal Ageing | | | |
|-----------------------|------------------------|--------------------------|----------------------|--------------------------|--------------------|-------------------|
| CoF | Tightening Torque [Nm] | Untightening Torque [Nm] | CoF Un-tightening | Untightening Torque [Nm] | Spacer Torque [Nm] | CoF Re-tightening |
| 0.118 | 17.6 | 15.1 | 0.4 | 26.9 | 12 | 0.24 |

Table 1: Comparison of Pre- and Post-Thermal Ageing Tests

Table 1 shows the torque measured for the joint prior to the thermal ageing process. As discussed this value was used to determine the torque required to achieve an end load of 11.6 kN with the spacer plate as opposed to the load cell in place. Figure 8 shows the torque profile of the joint both pre- and post-ageing. As shown in the figure, the torque required to turn the joint is significantly higher post-thermal ageing. This result, along with the torque attributable to rotation of the spacer, was used to estimate the thread friction (Table 1). As shown in the Table, the thread friction has increased significantly as a consequence of the thermal cycle, and has more than doubled in value.

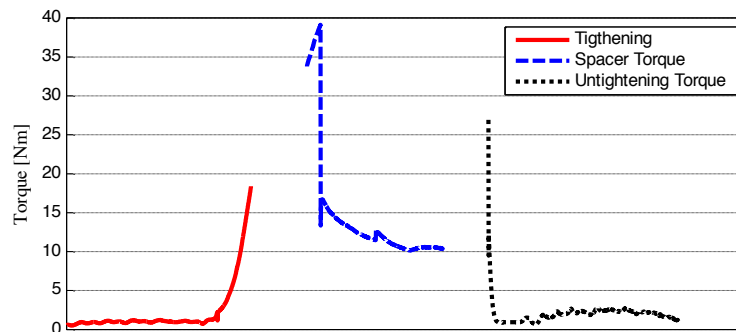


Figure 8: Torque during Thermal Ageing Test

As discussed, Figure 8 shows respectively the torque required to tighten the joint on the spacer, the torque required to rotate the spacer after ageing, and the torque required to unscrew the joint. The red curve shows the tightening torque, evaluated using the load cell, and used to re-assemble the joint with the spacer replacing the load sensor. The blue curve shows the torque required to rotate the spacer after the ageing process. When the spacer rotates relative to the joint, meaning both bearing surfaces slide. During the periodic engine maintenance, during unscrewing only one of them slides, either the bolt or the nut side, and in order to estimate the coefficient of thread friction only the total torque was halved. A peak torque was found at the beginning of the test, attributable to breaking the seizure that occurred with ageing, further highlighted by the washer-joint interfaces shown in Figure 9a. Finally, the black curve shows the untightening torque post-ageing, showing a higher torque than pre-ageing. During the test, silver removal and transfer to the mating threads and the spacer was also observed, and is shown in Figure 9b, with silver clearly evident on the bolt threads. As highlighted by this discussion, the coefficient of thread friction measured directly from the un-screwing process is indicative, and subject to a range of assumptions, with this going some way to explaining its difference in value to that measured once the joint is re-assembled.



Figure 9: a) Typical Washer-Joint Interface, b) Silver Transfer Post-Ageing

In order to further characterise the aged joints, once disassembled the joints were re-tested using the load cell. Figure 10a shows the torque and load curve for the aged joint compared to that for the cold test, further highlighting the increase in torque required to rotate the joint after the thermal cycle. Additionally, Figure 10b shows the coefficient of thread friction as a

function of joint load, where a similar increase in value with respect to load is once again evident, however, with a significantly higher overall value in the aged case, though less than determined from the aforementioned initial calculation (0.24 vs. 0.4 for re-assembly vs. unscrewing respectively (Table 1)).

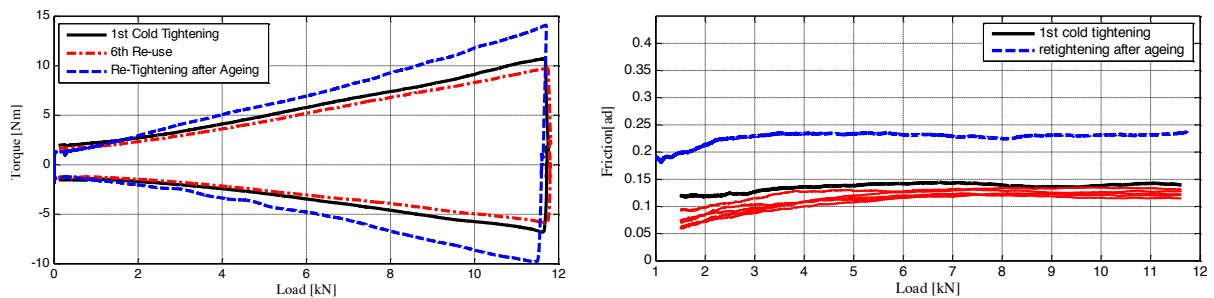


Figure 10: Pre- and Post-Heat Treatment (a) Load vs Torque Curve (b) Coefficient of friction

4 Finite Element Analysis

The tightening process is experimentally analysed by measuring the torque and the load, and calculating the coefficient of friction afterwards. However, the contact pressure and the stresses in the joints are not directly measured, thus a Finite Element approach was used to investigate the screwing mechanism of the self-locking fastener. The actual dimensions of the bolt, the nut and the load cell were used in the analysis, and whilst the silver coating was not represented as a different component, its interface behaviour were taken into account through the pressure dependent coefficient of friction used in the model. A 3D dynamic analysis of the joint was undertaken using the solver Simulia Abaqus 6.13 Standard 3D (Implicit) [15], with material properties as defined in Table 2.

| Part | Material | Density [kg/m ³] | Young's mod. [MPa] | Poisson's modulus | Plastic behaviour |
|-----------|----------------|------------------------------|--------------------|-------------------|-----------------------------------------------------------------|
| BOLT | Waspaloy | 7780 | 197000 | 0.27 | YES (isotropic hardening, true stress-true strain curve)[16] |
| NUT | | | | | |
| LOAD CELL | Stainless 17-4 | 8200 | 213000 | 0.29 | NO |

Table 2: Material Properties

A further boundary condition required was the frictional behaviour of the silver coating at the thread contacts. This was analysed using the ball on disc sliding test [17], using a ¼” Inconel ball and a 70mm silver coated disc at a speed of 1 mm/s at room temperature to reproduce the joint contact. Mobil Jet Oil II was once again used and different load cell were used in order to reach 1200MPa in the UMT tribometer. The test highlighted a pressure dependent relationship between the coefficient of friction and the contact pressure, where the coefficient of friction first decreased, before rising again with increasing pressure (Figure 11). As shown in the figure, the coefficient of friction results show some scatter at low contact pressure, with this attributable to the accuracy of the small load cell used in the pin on disc test machine at low values of applied load. In fact, three load cells were used during the test, such as 0.5, 5 and 200N, with an accuracy of 0.5% of the full scale and a minimum pressure achieved of 50MPa.

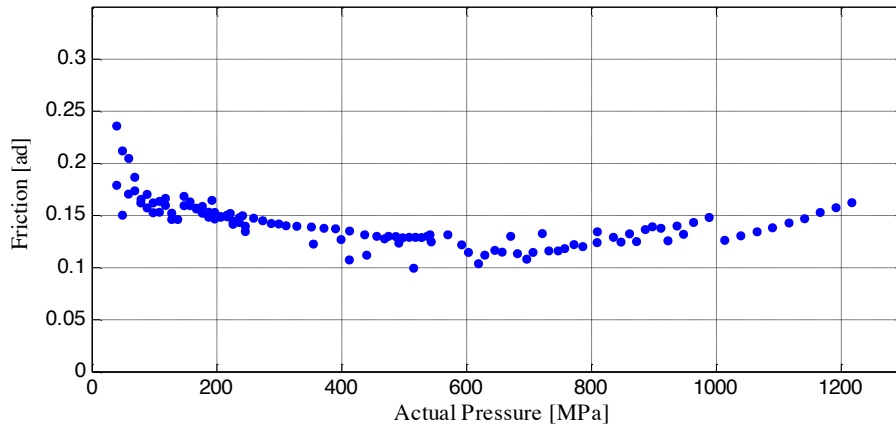


Figure 11: Coefficient of Friction in the Ball on Flat Test.

The friction along with the pressure was tabulated and used as an input in the FE model. The other surfaces in contact, such as the surface between the load cell and the bolt and nut under-head surface, were defined as frictionless, to reproduce the experimental conditions, where the bearing torque was subtracted from the total torque. Several additional assumptions were also made in order to reduce the solution time. For example, thermal effects as a result of high tightening speed and their potential impact on the frictional properties of silver were not considered, as experiments were performed at low speed. Furthermore, the surface roughness was not considered and chamfers far from the surfaces in contact in the nut and in the bolt were simplified in order to reduce the solving time. For the same reason, a course mesh was used to define the load cell, whilst still preserving the model accuracy. A mesh refinement process was done to maximise the efficiency of the simulation, increasing the number of elements in the area of interest, where hexa elements were used. In total, 235k elements and 87.5k nodes were used for the simulation.

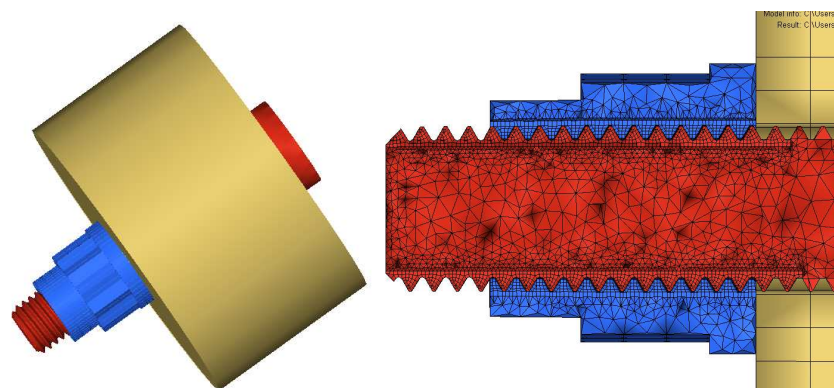


Figure 12: Finite Element parts

In the model crimping of the nut, winding on, and the final tightening of the joint were simulated. During this simulation, the torque and the clamping load were extracted and compared to the experimental results (Figure 13).

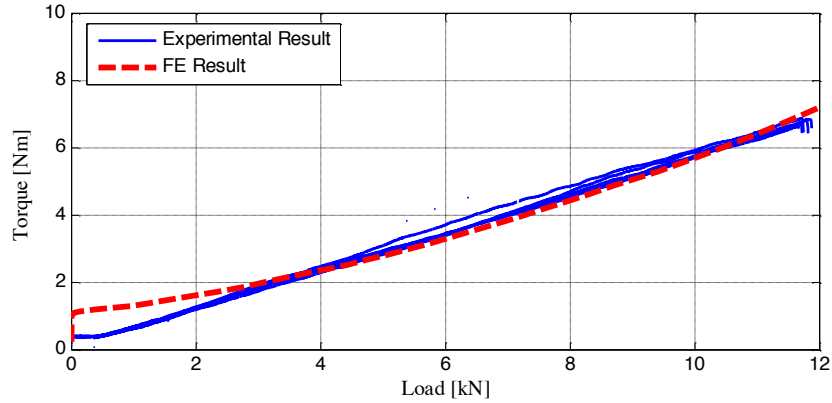


Figure 13: FE Model Validation

As shown in Figure 13, the FE result matched the experimental results, apart from for the first part of the clamping sequence, where a lack of friction data at low pressure was found to be an issue. Figure 14 shows the contact pressure distribution in the joint at a load of 1.32kN, and is a load case where the FE and experimental results differed. As shown in the figure, a significant percentage of the contact points experience a pressure lower than 150MPa, coinciding with the area of scatter in the ball on flat results for coefficient of friction.

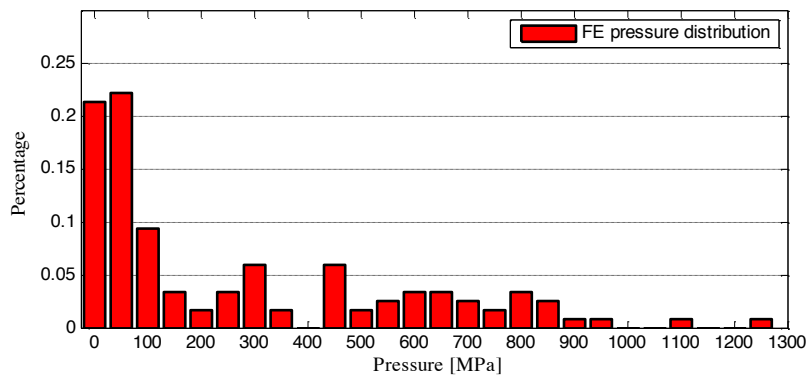


Figure 14: Pressure Distribution at 1.3kN

The Von Mises stress, the contact pressure and the deformations were analysed during the entire process, showing the maximum stress when the end load is reached. (Figure 15)

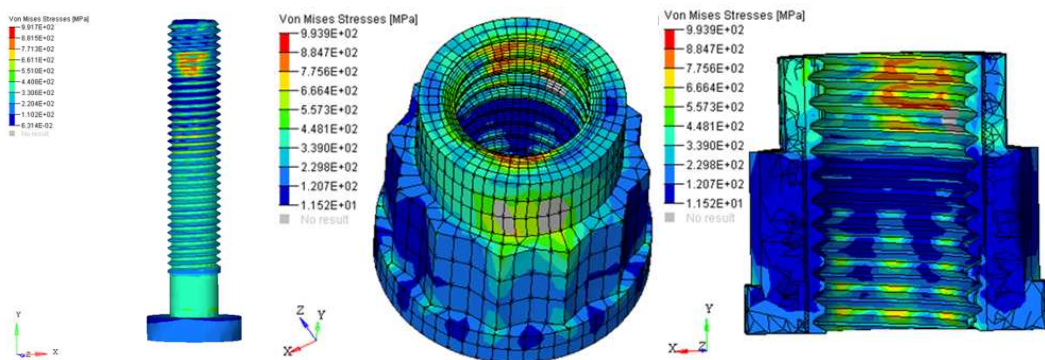


Figure 15: Von Mises stresses in the Joint

As shown in the figure, a maximum von Mises stress of 990 MPa is reached at the contact between the bolt and nut in the crimped section at the end load. Furthermore, the bolt was

stretched, as highlighted by the stresses along the shank and the threads, further validating the simulation. The stress distribution in the axial direction were analysed and plotted at different stages of the tightening process, in order to map the stresses as a function of the clamping load.

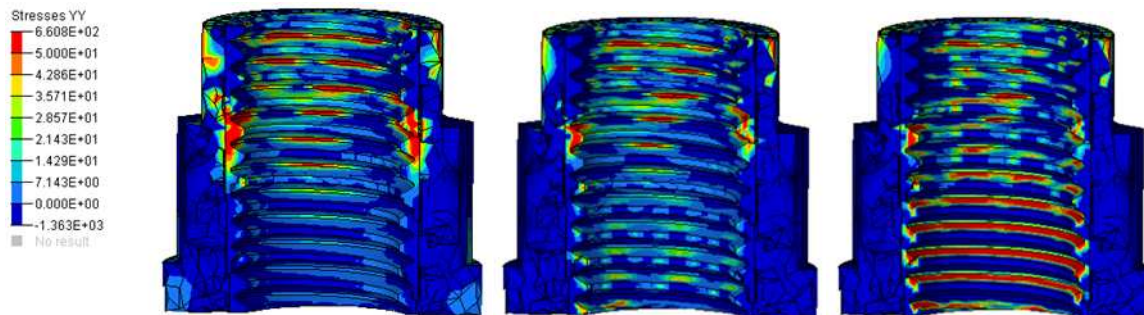


Figure 16: Axial Stresses at 1kN, 3kN and 11.6kN

As shown in Figure 16, the load is entirely taken by the crimped section until 3kN, when the first threads start to be loaded. At the end load of 11.6kN, the pressure is mainly in the first five revolutions, while in the crimp section the stresses are reduced, however, it still supports part of the load.

5 Discussion

Figure 12 compares the coefficient of friction from the experiment and simulation. In the experimental test, the coefficient of thread friction was calculated during the entire tightening process, and was found to be a function of the clamping load. As indicated in Equation 3, the coefficient of friction is calculated using thread torque and the clamping load at a given point in the clamping cycle. From the Finite Element Model the coefficient of friction has been calculated in two ways, firstly as an average on a nodal basis, and secondly by extracting the thread torque and the clamping load at a given tightening step and applying Equation 3.

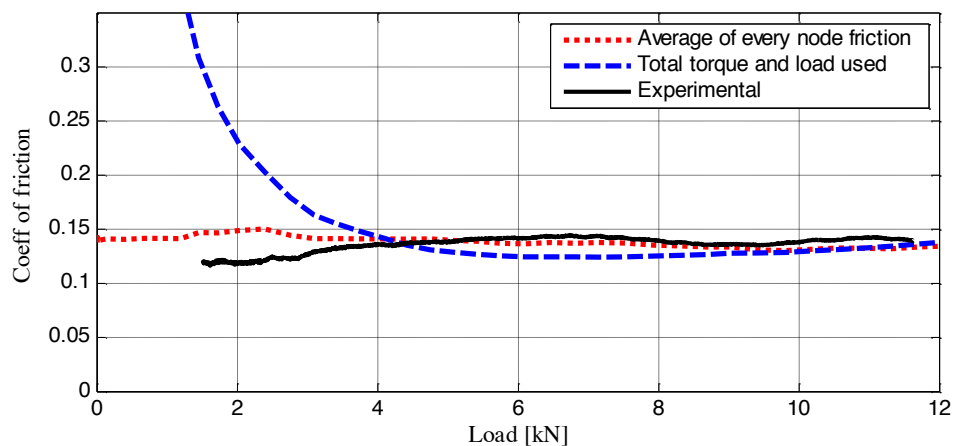


Figure 17: Coefficient of Friction during Tightening

As shown in Figure 17, the three curves are similar at high load, but show significant variation at lower load, and each have associated inaccuracies. For example, Equation 3 assumes a constant coefficient along the entire nut, disregarding the dependency of the pressure, a relationship clearly highlighted in the ball on flat test (Figure 11). This will lead to an error in the calculated coefficient of friction for both the experimental data and FE result using total load and torque, with this effect more pronounced at low clamping load where a

more significant variation in contact pressure along the nut has been identified. Similarly, the coefficient of friction data from the ball on flat test is inaccurate at low pressure, and will lead to inaccuracy in both of the finite element results at low load.

As previously described, the coefficient of thread friction calculated using the experimental torque and load was found to be a function of the clamping load, (Figure 6). This effect is best explained through the FE simulation, where the contact pressure in the threads was also found to increase with axial load, (Figure 16), and as highlighted by the ball on flat test leads to an increase in the coefficient of friction of silver (Figure 11). The result from the ball on flat test was also similar to that observed by Yang et al.[18], which analysed the tribological behaviour of the silver coating in a ball on flat test in a pressure range of 100-1000MPa, highlighting the wear and friction dependency with respect to pressure.

During the cold and ageing test some of the silver coating was removed from the substrate, mainly in the crimped section of the nut. In order to highlight the stripping process, different joints were split at different axial engagements, and the pattern of damage compared to the FE contact pressure distribution. As shown in Figure 18, the nuts were split when the first thread of the bolt was one, two and three revolutions out of the chimney.

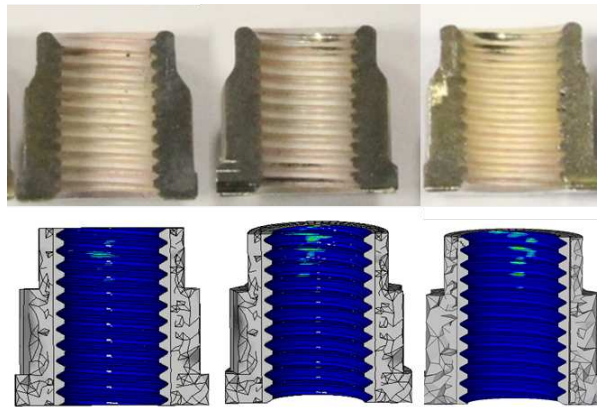


Figure 18: Comparison between Silver Removed during the Screwing Process and FE Results.

Clearly, the FE result matches the experimental result, with the silver removed in particular in the crimped section, where high contact pressures were identified. Furthermore, the comparison showed a contact pressure of approximately 750MPa lead the silver to strip.

As previously shown in Figure 10, during the ageing process the frictional behaviour of silver changes, with an increase recorded. To further analyse the effect of ageing on the properties of the coating, Hysitron Triboscope TS70, capable of a maximum load of 10mN and maximum roughness of 3.5 μ m, was used to measure the hardness both pre- and post-ageing. The measurements were recorded on the flat bearing surface of the nut, as the threads were found to be impracticable. The pre-aged samples were polished with 0.25 microns diamond suspension for 2 minutes before the first test, with a resulting roughness of 500-800nm (Figure 19a), and a coating thickness of 5.5-7 μ m. With a Berkovic indenter, a 10 cycle partial loading and unloading test was undertaken, with a maximum load of 10mN. Three locations on the sample were analysed, using a 3 by 3 matrix in a 50 μ m square scan area. The same measurements and test were undertaken on the aged samples. While the thickness of the coating was found to be almost the same, the roughness was higher at 3-4 μ m (Figure 19b), reaching the machine roughness limit. Furthermore, the hardness of the unpolished surface was measured and no significant change was found. Additionally, the coating hardness was measured before the polishing process showing no significant difference; however, the polishing process was found necessary in order to measure the hardness post-ageing, as this measurement was otherwise impossible due to the roughness limit in the machine.

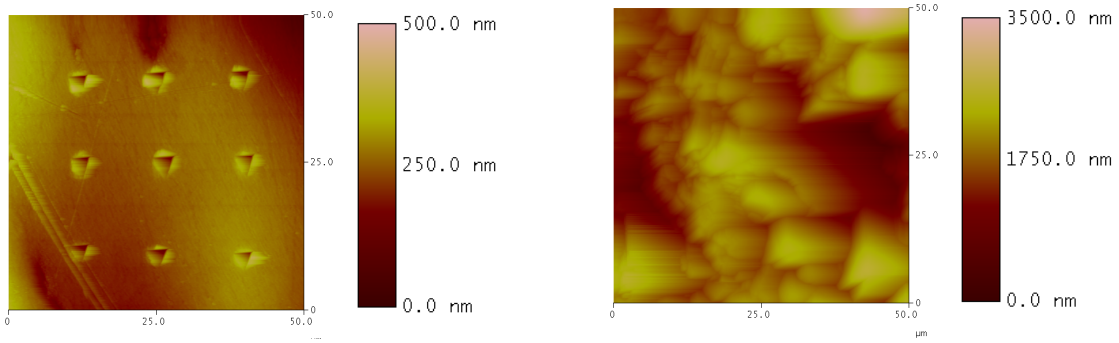


Figure 19: Comparison between Pre-aged (a) and Post-aged (b) Silver Coating

The hardness of the coated nut pre and post-ageing, automatically measured by the instrument from the partial unloading curve, was plotted and compared (Figure 20).

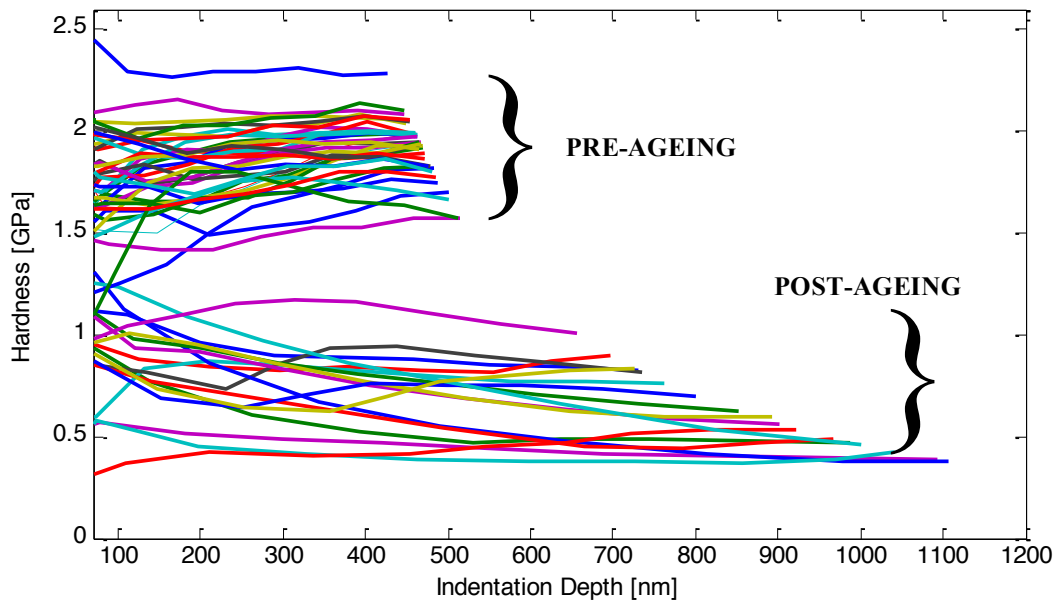


Figure 20: Silver Hardness Pre- and Post-ageing

As shown in Figure 20 the hardness of the pre-aged sample is between 1.4 and 2.3GPa, while the hardness of the post aged sample is lower, from 0.5 to 1.2GPa. This result clearly indicates that the ageing process anneals the silver, leaving it susceptible to removal at lower contact pressures. In order to further explore this effect, split nuts were compared from the cold re-use test (Figure 21a) and in the aged condition post-unscrewing (Figure 21b). As shown in the figures, a significant amount of silver has been removed post-ageing, as evidenced by the dark appearance in many places of the threads. As a consequence of the severe damage to the silver coating, an increase in the coefficient of friction is expected, as the contact becomes chemically similar to a like on like couple. Similar behaviour has also been explored by Roberts et al.[19], where softening and annealing of silver were considered in pin on disc tests. Additionally in tests at elevated temperature, the study also found no significant difference between tests in air and nitrogen atmospheres, further highlighting the oxidation resistance of silver coatings.

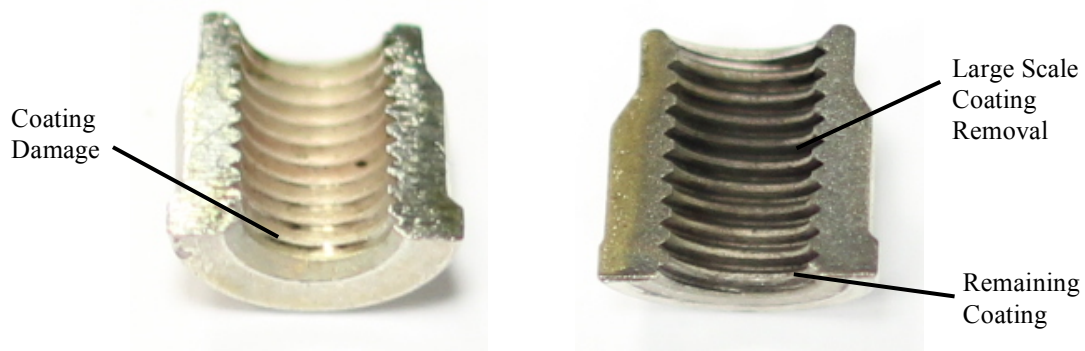


Figure 21: Sectioned silver nut (a) after cold use test and (b) after post-ageing test.

6 Conclusions

The analysis of the silver coating behaviour in aerospace fasteners was summarised as follows:

- The coefficient of friction has been determined for a silver coated crimped joint as it is tightened, showing a dependency on the end load.
- Thermal ageing of the joint led to a significant increase in the coefficient of friction.
- The entire process of tightening has been analysed through using a FE model, considering the self-locking feature and the pressure dependency of the coefficient of friction, and showed a good match with the experimental results.
- By combining the experimental and FE results, an insight into the behaviour of the silver coating was established, with shear flow and damage at higher contact pressures identified.
- The nano-hardness test showed annealing of the silver coating with thermal ageing, with a corresponding stripping of the silver coating, resulting in a like on like couple in the joint and an associated rise in coefficient of friction.

References

- [1] Juvinal RC, Marshek KM. *Fundamentals of Machine Component Design*. Wiley; 2006.
- [2] Junker GH. *New Criteria for Self-Loosening of Fasteners Under Vibration*. 1969. doi:10.4271/690055.
- [3] Pai NG, Hess DP. Experimental Study of Loosening of Threaded Fasteners Due To Dynamic Shear Loads. *J Sound Vib* 2002;253:585–602. doi:10.1006/jsvi.2001.4006.
- [4] Martínez M., Pantoja M, Abenojar J, Del Real JC, Velasco F. Influence of thread geometry on the performance of retaining anaerobic adhesives. *Int J Adhes Adhes* 2011;31:429–33. doi:10.1016/j.ijadhadh.2011.03.004.
- [5] Petrova a. P, Lukina NF. Adhesive technologies in aircraft construction. *Polym Sci Ser D* 2008;1:83–90. doi:10.1134/S1995421208020032.

- [6] Kumar SN. Investigation on the self loosening behavior of hexagonal nut and nylock nut in curvic coupling under transverse loading. IOSR J Mech Civ Eng n.d.:63–6.
- [7] Smith C. Carroll Smith's Nuts, Bolts, Fasteners and Plumbing Handbook: Technical Guide for Racer, Restorer and Builder. Motorbooks; 1990.
- [8] Houghton A. Use of Tribological Design and Surface Engineering to Improve Riser Valve Components 2015.
- [9] Houghton a., Lewis R, Olofsson U, Sundh J. Characterising and reducing seizure wear of inconel and incoloy superalloys in a sliding contact. Wear 2011;271:1671–80. doi:10.1016/j.wear.2011.02.022.
- [10] Holmberg K, Matthews A. Coatings Tribology: Properties, Mechanisms, Techniques and Applications in Surface Engineering. Elsevier; 2009.
- [11] Yang SH, Kong H, Yoon E-S, Kim DE. An experimental study on the rolling resistance of bearings coated by pure silver. Wear 1999;225-229:119–26. doi:10.1016/S0043-1648(98)00354-8.
- [12] El-Sherbiny M, Salem F. Tribological Properties of PVD Silver Films. A S L E Trans 1986;29:223–8. doi:10.1080/05698198608981681.
- [13] Bal Seal Engineering. Metal Plating Processes and Methods of Measuring Surface Hardness and Thickness of Coatings. 2003.
- [14] Dean S, Reiff J. A Procedure for Calculation of Torque Specifications for Bolted Joints with Prevailing Torque. J ASTM Int 2005;2:12879. doi:10.1520/JAI12879.
- [15] Abaqus 6.13 Documentation. Dassault Systèmes; 2013.
- [16] Atlas of Stress-strain Curves. ASM International; 2002.
- [17] Astm. ASTM G99: Standard Test Method for Wear Testing with a Pin-on-Disk Apparatus. ASTM Stand 2010;G99:1–5. doi:10.1520/G0099-05R10.2.
- [18] Yang SH, Kong H, Yoon ES, Kim DE. A wear map of bearing steel lubricated by silver films. Wear 2003;255:883–92. doi:10.1016/S0043-1648(03)00148-0.
- [19] Pauleau Y. Protective Coatings and Thin Films: Synthesis, Characterization, and Applications. Springer Science & Business Media; 1996.